

Reliable quantum kernel classification using fewer circuit evaluations

Abhay Shastry,^{*} Abhijith J.,[†] Apoorva Patel,[‡] and Chiranjib Bhattacharyya^{*}
(Dated: October 14, 2022)

Quantum kernel methods are a candidate for quantum speed-ups in supervised machine learning. The number of quantum measurements N required for a reasonable kernel estimate is a critical resource, both from complexity considerations and because of the constraints of near-term quantum hardware. We emphasize that for classification tasks, the aim is accurate classification and not accurate kernel evaluation, and demonstrate that the former is more resource efficient. In general, the uncertainty in the quantum kernel, arising from finite sampling, leads to misclassifications over some kernel instantiations. We introduce a suitable performance metric that characterizes the robustness or reliability of classification over a dataset, and obtain a bound for N which ensures, with high probability, that classification errors over a dataset are bounded by the margin errors of an idealized quantum kernel classifier. Using techniques of robust optimization, we then show that the number of quantum measurements can be significantly reduced by a robust formulation of the original support vector machine. We consider the SWAP test and the GATES test quantum circuits for kernel evaluations, and show that the SWAP test is always less reliable than the GATES test for any N . Our strategy is applicable to uncertainty in quantum kernels arising from *any* source of noise, although we only consider the statistical sampling noise in our analysis.

I. INTRODUCTION

Kernel methods have been used extensively in a variety of machine learning tasks like classification, regression, and dimensionality reduction [1]. The core ingredient of such algorithms is the so-called kernel trick, which implicitly embeds a data point into a higher (possibly infinite) dimensional inner product space, known as the *feature space*. The embedding is implicit because the vectors in the feature space are never explicitly computed. Instead, a *kernel function* is used to map any two input data points to the inner product between their embeddings in the feature space. The key insight that allows kernel methods to be used with quantum computers is the identification of a vector in the feature space with the density matrix of a many-body quantum system [2, 3].

Quantum computing allows us to efficiently compute the inner products of exponentially large density matrices without the explicit computation of the density matrices themselves. Naturally, such an extension into the quantum setting has interested researchers to search for a quantum advantage in kernel methods [4–8]. In particular, Ref. [4] analyses the spectral properties of the reproducing kernel Hilbert space (RKHS) associated with a quantum density matrix and suggests that a quantum advantage can be expected if the RKHS is low-dimensional and has functions which are classically hard to compute. This can however lead to a situation where the quantum kernel evaluation requires an exponentially large number of measurements, thereby making it hard to claim quantum advantage. The number of measurements N needed

for a kernel evaluation thus plays an important role in the analysis of quantum algorithms for machine learning.

In the present article, we look at the problem of quantum kernel classification with particular emphasis on optimization of N . Suppose a kernel function K^* , which may be classically hard to compute, has to be implemented on a quantum machine. How many measurements would be needed to construct a reliable classifier? Crucially, our goal is *not* to accurately evaluate the kernel function itself but to construct a reliable classifier with it. It is often possible to have a training dataset with few support vectors m_{sv} [9], which do not scale with the number of training data points m . Physically, $m_{sv} \ll m$ is essentially a boundary (support vectors) vs. bulk (all datapoints) comparison. In a Support Vector Machine (SVM), the boundary carries the information relevant to the classifier. Faithful reproduction of the training labels is shown to require $N = \Omega(m_{sv} \log m)$ measurements per kernel entry. In contrast, bounds for N derived over the error ϵ (in operator distance) in the training kernel matrix [5, 10], $N = \Omega(m^2/\epsilon^2)$, scale quadratically with m .

We work in the hybrid quantum-classical setup [2, 5, 11], where the optimization problem is solved on a classical machine and the kernel evaluations are done on a quantum machine by repeated measurements of a quantum logic circuit. In setting up the optimization problem, we assume that we have access to the kernel matrix \mathbf{K}^* over the training data. We refer to quantum classifiers which use N measurements of a quantum circuit per kernel evaluation as *stochastic kernel classifiers* (SKC), and the ideal quantum classifier ($N \rightarrow \infty$) as the *exact kernel classifier* or the *true classifier* (EKC). Our aim is to reliably reproduce the output of the exact kernel classifier using as few measurements as possible. In the results presented in this article, we test the classifier over the training data itself. This choice highlights the problem starkly, since it shows that the stochastic kernel classifiers are incapable of reliably reproducing *even the*

^{*} Department of Computer Science and Automation, Indian Institute of Science, Bangalore 560012

[†] Theoretical Division, Los Alamos National Lab, New Mexico, US 87545

[‡] Center for High Energy Physics, Indian Institute of Science, Bangalore 560012

training labels, when N is not large enough. We show its generalization to an independent test set in the Supplementary Information (Supp. Info.). Our main findings are summarized in the next two paragraphs.

In Section V A, we derive a bound for N (Theorem 2) which ensures (with high probability) that the classification error of the SKC is smaller than the margin error of the EKC over any dataset. This constitutes a more useful bound than the ones derived over the errors in the training kernel matrix [5, 8, 10], since the latter do not have any direct relationship with the performance of the classifier. The bound is based on the observation that when the effect of the kernel uncertainty is smaller than the margin of classification, the classifier results do not change.

In Section V B, we take a chance constraint approach [12] to handle the stochastic parts of the SVM objective [13], and develop a convex cone program which is robust to the sampling noise by construction (Theorem 3). Solving this robust optimization problem allows us to construct two classifiers, *robust stochastic kernel classifier* (RSKC) and *robust exact kernel classifier* (REKC). The former employs the stochastic kernel and the latter employs the true quantum kernel for classification. We show that the sampling noise affects RSKC to a far lesser degree than the SKC. In particular, our construction of the robust SVM objective is such that even for single-shot measurements ($N = 1$) RSKC reliably reproduces REKC, although there is a corresponding trade-off in the accuracy of REKC for low N . Increasing N , we show that RSKC reproduces the true quantum classifier EKC with significantly less measurements per kernel entry compared to SKC. This result is especially relevant for the current noisy intermediate-scale quantum (NISQ) era [14] quantum devices, where the number of measurement shots are a resource to be used frugally [15–17].

II. PRELIMINARIES

In this Section we introduce the relevant notation and discuss necessary preliminaries.

Notation The set of natural numbers is denoted by \mathbb{N} . For any $m \in \mathbb{N}$, $[m]$ denotes the set $\{1, \dots, m\}$. \mathbb{R}^d denotes a d dimensional real vector space. For any $\mathbf{v} \in \mathbb{R}^d$, the euclidean norm is $\|\mathbf{v}\| = \sqrt{\mathbf{v}^\top \mathbf{v}}$. A random variable $X \in \mathbb{R}^d$ distributed according to probability distribution \mathcal{P} is denoted as $X \sim \mathcal{P}$, and its expectation value denoted as $\mathbb{E}(X)$. The binomial random variable is denoted by $\text{Bin}(N, p)$, where $N \in \mathbb{N}$ is the number of independent Bernoulli trials each with success probability $0 \leq p \leq 1$. The number of quantum measurements or circuit evaluations (per kernel estimation) is denoted by N . The size of the training set is denoted by m . \mathbb{S}_+^m denotes the space of $m \times m$ positive semidefinite and symmetric matrices.

Definition 1 (Subgaussian random variable). *A random*

variable $X \in \mathbb{R}$ is $X \sim \text{SubG}(\sigma^2)$, if $\mathbb{E}(X) = 0$ and

$$\mathbb{E}(e^{sX}) \leq e^{\frac{1}{2}s^2\sigma^2} \quad \forall s \in \mathbb{R} \quad (1)$$

The smallest such σ is called the subgaussian norm of X .

The following facts about subgaussian random variables will be used subsequently.

Fact 1. Define $Z = \frac{1}{N}X - p$, where $X \sim \text{Bin}(N, p)$. Then $Z \sim \text{SubG}(\sigma^2)$ for any $\sigma^2 \geq \text{Var}(Z)$.

Fact 2. Subgaussian random variables obey the following tail bounds [18]:

1. If $X \sim \text{SubG}(\sigma^2)$ then for every $t > 0$,

$$\text{Prob}(X \geq t) \leq \exp\left(-\frac{t^2}{2\sigma^2}\right).$$

2. Let $X_i \sim \text{SubG}(\sigma^2)$, $i \in [n]$ be independent random variables. Then for any $a \in \mathbb{R}^d$ the random variable $Y = \sum_{i=1}^n a_i X_i$ satisfies

$$\text{Prob}(Y \geq t) \leq \exp\left(-\frac{t^2}{2\sigma^2\|a\|^2}\right). \quad (2)$$

This immediately leads to the following assertion.

Lemma 1. Let Y be defined as in Fact 2. For any $0 < \delta \leq 1$,

$$\text{Prob}(Y \geq t) \leq \delta \quad (3)$$

holds whenever

$$t \geq \sigma \|a\| \kappa(\delta),$$

where

$$\kappa(\delta) = \sqrt{2 \log\left(\frac{1}{\delta}\right)}. \quad (4)$$

A. Support Vector Machines for Classification

A function $f : \mathcal{X} \subset \mathbb{R}^d \rightarrow \{-1, 1\}$ is called a binary classifier, which takes an *observation* \mathbf{x} and outputs a label y . The problem of estimating f from a training dataset

$$\mathcal{D}_{\text{train}} = \{(\mathbf{x}_i, y_i) \mid \mathbf{x}_i \in \mathcal{X} \subset \mathbb{R}^d, y_i \in \{-1, 1\}, i \in [m]\} \quad (5)$$

consisting of m i.i.d. (*observation, label*) pairs drawn from a distribution \mathcal{P} is of great interest in machine learning. The aim is to obtain an f such that the generalization error, $\text{Prob}(f(\mathbf{x}) \neq y)$, is small for $(\mathbf{x}, y) \sim \mathcal{P}$.

Support Vector Machines (SVM) are widely used classifiers [19], which have been extremely successful in practical applications. For a dataset $\mathcal{D}_{\text{train}}$, a SVM kernel classifier is

$$f(\mathbf{x} \mid \alpha, b; K) = \text{sgn}\left(\sum_{i=1}^m \alpha_i y_i K(\mathbf{x}_i, \mathbf{x}) + b\right),$$

where the $\alpha = [\alpha_1, \dots, \alpha_m]^\top$ is obtained by solving the problem

$$\begin{aligned} \max_{\alpha} & \left(\sum_{i=1}^m \alpha_i - \frac{1}{2} \sum_{i,j} \alpha_i \alpha_j y_i y_j K(\mathbf{x}_i, \mathbf{x}_j) \right), \quad (\text{DUAL}) \\ \text{s.t.} & \sum_{i=1}^m \alpha_i y_i = 0 \text{ and } 0 \leq \alpha_i \leq C, \end{aligned}$$

for some $C \geq 0$.

This optimization problem can be solved efficiently using convex quadratic programming [1]. The kernel function $K : \mathcal{X} \times \mathcal{X} \rightarrow \mathbb{R}$ is *positive semidefinite*, and plays the role of a dot product in a suitably defined Reproducing Kernel Hilbert Space (RKHS). One of the most interesting properties of the kernel function is it implicitly defines an embedding of the observation that does not need to be explicitly computed. For a comprehensive exposition, see Ref. [20]. For brevity we introduce the kernel matrix $\mathbf{K} \in \mathbb{R}^{m \times m}$, whose entries are $\mathbf{K}_{ij} = K(\mathbf{x}_i, \mathbf{x}_j)$ for any $i, j \in [m]$. Since the kernel function is positive semidefinite, the kernel matrix is also positive semidefinite.

To help develop our ideas, we work with an equivalent setup. We consider classifiers of the form

$$f(\mathbf{x}|\beta, b; K) = \text{sgn} \left(\sum_{i=1}^m \beta_i K(\mathbf{x}_i, \mathbf{x}) + b \right), \quad (6)$$

where $\beta = [\beta_1, \dots, \beta_m]^\top \in \mathbb{R}^m, b \in \mathbb{R}$. The parameters β, b of the classifier are obtained by minimizing

$$\begin{aligned} J(\beta, b; \mathbf{K}) = C \sum_{i=1}^m \max & \left(1 - y_i \left(\sum_{j=1}^m \beta_j \mathbf{K}_{ij} + b \right), 0 \right) \\ & + \frac{1}{2} \sum_{ij} \beta_i \beta_j \mathbf{K}_{ij}, \end{aligned} \quad (7)$$

for some $C \geq 0$ (same as in DUAL) that sets the relative weights of the two terms. The first term is known as the hinge loss, and the second term is called the regularization term. Since the kernel function is positive semidefinite, this is a convex quadratic function. The resulting problem,

$$\min_{\beta \in \mathbb{R}^m, b \in \mathbb{R}} J(\beta, b; \mathbf{K}), \quad (\text{PRIMAL})$$

is thus again a convex optimization problem, and is dual to the standard SVM formulation.

B. Quantum Embedding Kernels

Kernel methods have a natural extension into the quantum setting. A quantum computer can be used to embed the data into a high dimensional Hilbert space and the kernel function can be computed by estimating

the state overlaps. This also offers a path to obtain quantum advantage in machine learning, since certain type of kernel functions are (conjectured to be) hard to evaluate classically but easy to do so quantum mechanically [4–6]. A quantum embedding circuit takes the classical input datapoint $\mathbf{x} \in \mathcal{X} \subset \mathbb{R}^d$, and maps it to a quantum state $|\phi(\mathbf{x})\rangle \in \mathcal{H}$, the *computational* Hilbert space. A valid kernel function $K : \mathcal{X} \times \mathcal{X} \rightarrow \mathbb{R}$ can be chosen as

$$K(\mathbf{x}, \mathbf{x}') \equiv \text{Tr} \{ \rho(\mathbf{x}) \rho(\mathbf{x}') \} = |\langle \phi(\mathbf{x}) | \phi(\mathbf{x}') \rangle|^2, \quad (8)$$

where $\rho(\mathbf{x}) \equiv |\phi(\mathbf{x})\rangle \langle \phi(\mathbf{x})|$ is the density matrix that plays the role of a vector in the feature Hilbert space $\mathcal{H} \otimes \mathcal{H}^*$. Such kernels are known as *quantum embedding kernels* (QEK) [2, 3].

The mapping into the computational Hilbert space $|\phi(\mathbf{x})\rangle = U(\mathbf{x})|0\rangle^n$ is achieved by a unitary operator $U(\mathbf{x})$ using a quantum circuit dependent on \mathbf{x} . For example, we may use the elements of \mathbf{x} as the angles of rotation in the various 1- and 2-qubit gates used to construct the quantum circuit. Such an angle embedding circuit is shown in Supp. Info., and is one of the simplest ways to encode the input data \mathbf{x} into a quantum state $|\phi(\mathbf{x})\rangle$. Given such a circuit, we can map each datapoint to a quantum density matrix, $\rho(\mathbf{x}) = U(\mathbf{x})|0 \dots 0\rangle \langle 0 \dots 0| U^\dagger(\mathbf{x})$. The kernel can then be expressed as the Hilbert-Schmidt inner product $K(\mathbf{x}, \mathbf{x}') = \text{Tr} \{ \rho(\mathbf{x}) \rho(\mathbf{x}') \}$, which can be evaluated using either the SWAP test or the GATES circuit that we describe in the next Section.

III. THE QUANTUM SAMPLING NOISE IN KERNEL EVALUATIONS

Let K^* denote the true quantum kernel function and $K^{(N)}$ be the stochastic kernel function estimated from N quantum measurements for any pair of inputs $\mathbf{x}_i, \mathbf{x}_j \in \mathcal{X}$. We shall use the shorthand notation $K_{ij}^* = K^*(\mathbf{x}_i, \mathbf{x}_j)$ and $K_{ij}^{(N)} = K^{(N)}(\mathbf{x}_i, \mathbf{x}_j)$. We denote their difference at finite sampling as

$$\Delta K_{ij}^{(N)} = K_{ij}^* - K_{ij}^{(N)}, \text{ for any } \mathbf{x}_i, \mathbf{x}_j \in \mathcal{X}. \quad (9)$$

In what follows, we demonstrate that the sampling noise depends on the quantum logic circuit used to evaluate the kernel function.

We consider the two different ways in which the overlaps $K_{ij} = |\langle \phi(\mathbf{x}_i) | \phi(\mathbf{x}_j) \rangle|^2$ can be evaluated [5]. The data $\mathbf{x}_i \in \mathcal{X}$ is transformed into a state in the computational Hilbert space \mathcal{H} by starting with all n qubits in the $|0\rangle$ state and using the unitary operator

$$|\phi(\mathbf{x}_i)\rangle = U(\mathbf{x}_i)|0\rangle^{\otimes n}. \quad (10)$$

The first method is to express the kernel as $K(\mathbf{x}_i, \mathbf{x}_j) = |\langle 0|^{\otimes n} U^\dagger(\mathbf{x}_i) U(\mathbf{x}_j) |0\rangle^{\otimes n}|^2$, which can be evaluated by applying $U^\dagger(\mathbf{x}_i) U(\mathbf{x}_j)$ to the initial state $|0\rangle^{\otimes n}$ and then estimating the probability that the final state is also $|0\rangle^{\otimes n}$. We refer to this as the GATES test, shown in fig.

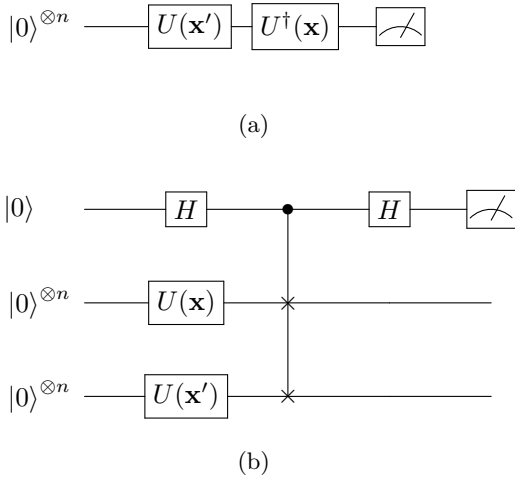


FIG. 1: (a) GATES circuit measures the probability of obtaining the final state $|0\rangle^{\otimes n}$. The resulting distribution for $K(\mathbf{x}, \mathbf{x}')$ is given by (GATES). (b) SWAP circuit measures the probability of obtaining the ancillary qubit (top line) in the $|0\rangle$ state. The resulting kernel estimate is given by (SWAP).

1(a). It has also been called the inversion test [21] and the adjoint test [10]. The value of the kernel function $K_{ij}^{(N)} = K^{(N)}(\mathbf{x}_i, \mathbf{x}_j)$ is inferred using N independent Bernoulli trials, each of which gives the final state $|0\rangle^{\otimes n}$ with probability $p = K_{ij}^*$. Hence,

$$K_{ij}^{(N)} \sim \frac{1}{N} \text{Bin}\left(N, p = K_{ij}^*\right). \quad (\text{GATES})$$

An alternate way to measure fidelity or state overlap is the SWAP test [22], shown in fig. 1(b). In this case, the ancilla bit is read out, and the probability of obtaining the state $|0\rangle$ can be written in terms of the state overlap

$$\text{Prob}(\text{ancilla} = |0\rangle) = \frac{1}{2}(1 + |\langle \phi(\mathbf{x}_i) | \phi(\mathbf{x}_j) \rangle|^2) \quad (11)$$

$$= \frac{1}{2}(1 + K_{ij}^*). \quad (12)$$

We infer $K_{ij}^{(N)}$ through N independent Bernoulli trials that measure the state of the ancilla bit, and therefore obtain

$$K_{ij}^{(N)} \sim \frac{2}{N} \text{Bin}\left(N, p = \frac{1}{2}(1 + K_{ij}^*)\right) - 1. \quad (\text{SWAP})$$

In all the figures, we use the symbol (►) and (✖) to denote the (GATES) and (SWAP) tests respectively.

It is obvious that in both (GATES) and (SWAP) cases $K_{ij}^{(N)}$ is an unbiased estimator of K_{ij}^* ,

$$\mathbb{E}[K_{ij}^{(N)}] = K_{ij}^* \quad \forall \mathbf{x}_i, \mathbf{x}_j \in \mathcal{X}. \quad (13)$$

The variance of the estimator, however, is linked to the specific circuit and the number of measurements N .

Lemma 2 (Circuit Factor). *The variance of estimator $K_{ij}^{(N)}$ is upper-bounded by σ_0^2 , where*

$$\sigma_0 = \frac{c}{2\sqrt{N}}, \quad c = \begin{cases} 1 & (\text{GATES}), \\ 2 & (\text{SWAP}). \end{cases} \quad (14)$$

The circuit factor c is a circuit-dependent constant.

For a derivation of the σ_0 value, see Supp. Info. II. For both the circuits under consideration, $K_{ij}^{(N)}$ is an affine function of a Binomial random variable. Direct application of Fact 1 then yields

$$\Delta K_{ij}^{(N)} \sim \text{SubG}(\sigma_0^2). \quad (\text{UM})$$

We study the problem of kernel based classification under this uncertainty model, and only consider the fundamental sampling noise. We however note the following in the presence of other sources of noise, and discuss the modification to the uncertainty model in Supp. Info.

Remark 1. *The uncertainty model UM subsumes all other sources of noise as well.*

Proof. Since all quantum kernel distributions $0 \leq K(\mathbf{x}, \mathbf{x}') \leq 1$ have finite support, it is subgaussian due to Hoeffding's lemma (e.g. see 2.6 in [23]). \square

We note that the kernel estimate given by (GATES) has a lower variance compared to the estimate given by (SWAP). This implies that, purely from the perspective of sampling noise, the GATES test is preferable for any N . The GATES test requires a circuit whose depth is twice that of the SWAP test, but the SWAP test requires twice the number of qubits as the GATES test and additional controlled SWAP operations. The practical choice of the test to use for estimating QEKs can therefore depend on other factors like the coherence times and the quality of the gates available. For example, a recent study [24] on the IBM quantum hardware has shown that SWAP test is a poor choice compared to the GATES test for estimating QEKs, owing to errors in the controlled SWAP implementation. However, it appears that the authors have overlooked the fundamental statistical reason (lemma 2) in their comparison of the GATES and SWAP tests.

We next highlight the effect of finite N on the SVM classification problem, and motivate the performance metric of reliability as opposed to average accuracy.

IV. RELIABILITY OF QUANTUM KERNEL CLASSIFIERS

Problem Setup:

1. We work in the hybrid quantum-classical setup where the SVM is trained on a classical machine. It is assumed that we have access to the true training

kernel matrix $\mathbf{K}^* \in \mathbb{S}_+^m$. The optimal coefficients minimizing $J(\beta, b; \mathbf{K}^*)$ in (PRIMAL) are denoted by β^*, b^* and are determined on a classical machine.

2. The kernel function $K^{(N)}$, used in the classification of an observation $\mathbf{x} \in \mathcal{X}$ is evaluated using N measurements per kernel entry $K^{(N)}(\mathbf{x}, \mathbf{x}_i)$, $i \in [m]$ on a quantum machine using one of the circuits in Fig. 1. We assume no other noise sources apart from the fundamental sampling noise. After the evaluation of the kernel function, the classification is done on the classical machine by computing $f(\mathbf{x}|\beta^*, b^*; K^{(N)})$ (Eq. 6).

Thus we compare the following two classifiers:

Definition 2 (Exact Kernel Classifier). *The exact kernel classifier or the true classifier is*

$$f^*(\mathbf{x}) = f(\mathbf{x}|\beta^*, b^*; K^*), \quad (\text{EKC})$$

where β^*, b^* denote the optimal coefficients minimizing the (PRIMAL) objective $J(\beta, b; \mathbf{K}^*)$.

Definition 3 (Stochastic Kernel Classifier). *Let N denote the number of measurements performed to estimate the kernel function $K(\mathbf{x}, \mathbf{x}_i)$, for each $i \in [m]$. Then*

$$f^{(N)}(\mathbf{x}) = f(\mathbf{x}|\beta^*, b^*; K^{(N)}), \quad (\text{SKC})$$

where, as in (EKC), β^*, b^* denote the optimal coefficients minimizing the (PRIMAL) objective $J(\beta, b; \mathbf{K}^*)$.

Naturally, we would recover the true classifier (EKC) in the limit of infinitely many measurements:

$$\lim_{N \rightarrow \infty} f^{(N)}(\mathbf{x}) = f^*(\mathbf{x}). \quad (15)$$

But the convergence can be slow in practice, and would depend on the dataset and choice of the kernel function K^* .

Classifier performance over a dataset is generally quantified by its accuracy.

Definition 4 (Accuracy). *The accuracy of a classifier $f(\mathbf{x})$ over a dataset $\mathcal{D} = \{(\mathbf{x}_i, y_i), i \in [M]\}$,*

$$\text{Acc}(f) = \frac{1}{M} \sum_{i=1}^M \mathbb{1}_{f(\mathbf{x}_i)=y_i}, \quad (16)$$

is the fraction of datapoints classified correctly.

When $f(\mathbf{x}) = f^{(N)}(\mathbf{x})$ is a stochastic kernel classifier, the classification of any datapoint $\mathbf{x} \in \mathcal{X}$ depends upon the evaluation of kernels $K^{(N)}(\mathbf{x}, \mathbf{x}_i)$, $i \in [m]$ which are random variables. The accuracy (16) is thus also a random variable and is therefore not a suitable performance metric.

Given some datapoint $\mathbf{x} \in \mathcal{X}$, we would like the classifier (SKC) to return the same label as (EKC) with high probability.

Definition 5 (Reliability of quantum classifier).

Let $f^{(N)}$ denote a stochastic kernel classifier where the quantum kernels are evaluated with N measurements per entry. We say the reliability of the stochastic kernel classifier (SKC) at the datapoint $\mathbf{x} \in \mathcal{X}$ is at least $1 - \delta$, if

$$\mathcal{R}(\mathbf{x}; f^{(N)}, f^*) \equiv \text{Prob}\left(f^{(N)}(\mathbf{x}) = f^*(\mathbf{x})\right) \geq 1 - \delta, \quad (17)$$

where $f^*(\mathbf{x})$ denotes the true classifier (EKC).

When classifying the datapoint $\mathbf{x} \in \mathcal{X}$ using quantum kernels, we thus seek N that gives $\delta \ll 1$.

Theorem 1. *Let $g^*(\mathbf{x}) = \sum_j \beta_j^* K^*(\mathbf{x}, \mathbf{x}_j) + b^*$. The stochastic kernel classifier $f^{(N)}(\mathbf{x})$ agrees with the exact kernel classifier $f^*(\mathbf{x}) = \text{sgn}(g^*(\mathbf{x}))$ (EKC), with probability at least $(1 - \delta)$, whenever*

$$N \geq \frac{1}{2} \left(\frac{c \|\beta^*\|}{g^*(\mathbf{x})} \right)^2 \log \left(\frac{1}{\delta} \right), \quad (18)$$

where c is the circuit factor.

Proof. This bound is a direct application of lemma 1, along with the uncertainty model for quantum kernel classifiers (UM). \square

We provide the following empirical metric to quantify the reliability (17) over a number of trials. Let $f^{(N)}\{1\}, f^{(N)}\{2\}, \dots, f^{(N)}\{N_{\text{trials}}\}$ denote the specific instantiations of a stochastic classifier (SKC) over N_{trials} different trials.

1. For a given input datapoint (\mathbf{x}, y) , the stochastic kernel classifier $f^{(N)}$ has an empirical reliability

$$\hat{\mathcal{R}}(\mathbf{x}; f^{(N)}, f^*) = \frac{1}{N_{\text{trials}}} \sum_{k=1}^{N_{\text{trials}}} \mathbb{1}_{f^{(N)}\{k\}(\mathbf{x})=f^*(\mathbf{x})}, \quad (19)$$

with respect to that of the true classifier f^* .

2. We extend the notation above and define the empirical reliability over a dataset \mathcal{D} ($|\mathcal{D}| = M$) as

Definition 6 (Empirical Reliability).

$$\hat{\mathcal{R}}(f^{(N)}, f^*) = \frac{1}{M} \sum_{s=1}^M \mathbb{1}_{\hat{\mathcal{R}}(\mathbf{x}_s; f^{(N)}, f^*)=1}. \quad (20)$$

Thus, an observation \mathbf{x} is considered to be *reliably classified*, if the stochastic kernel classifier assigns it the same label for *all* N_{trials} instantiations. (We find that relaxing this requirement of the same label for N_{trials} instantiations to $N_{\text{trials}}(1 - \delta)$ instantiations hardly affects our results.) Henceforth, Eq. (20) shall simply be referred to as reliability. Over any dataset, it quantifies the fraction of points which are classified reliably. In our experiments, we set $N_{\text{trials}} = 200$.

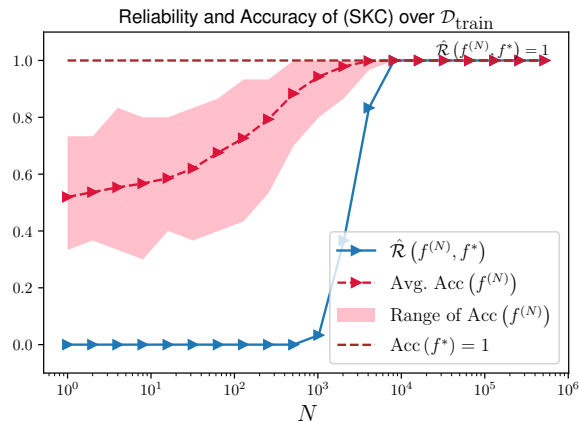


FIG. 2: **Reliability versus Accuracy.** Performance of (SKC) over the training dataset $\mathcal{D}_{\text{train}}$ shown as a function of N . Both quantities $\hat{\mathcal{R}}(f^{(N)}, f^*)$ and $\text{Acc}(f^{(N)})$ are calculated over the same $N_{\text{trials}} = 200$ instantiations of the kernel function $K^{(N)}$, using the (GATES) circuit and the Circles dataset. Accuracy itself is a random variable and the shaded area covers the range of observed accuracies of (SKC). Notice that even when the average accuracy is high ($> 85\%$ at $N = 512$), the reliability can be very low (0% at $N = 512$).

Reliability versus Accuracy:

An illustration of our numerical experiments is shown in FIG. 2. We observe that a large number of measurements are needed for (SKC) to reliably reproduce the labels *even for the training data*. Furthermore,

1. The *average* accuracy is not a good performance metric. A high accuracy on average carries little information regarding how *reliably* an observation \mathbf{x} is classified by (SKC). There is a wide range of the obtained accuracies over different instantiations of (SKC). For example, the average accuracy $> 85\%$ for $N = 512$, but *none* of the points are classified reliably.
2. Requiring high reliability, $\hat{\mathcal{R}}(f^{(N)}, f^*) \rightarrow 1$, as opposed to high accuracy on average, requires larger N .

In NISQ devices, the effect of noise on the results is extremely important and has received wide attention [14]. Recent works in quantum algorithms for the NISQ era place special emphasis on the sampling noise, and treat the number of measurements N as a resource that should be used minimally [15–17].

There exists however a large discrepancy in the number of measurements used in various studies of quantum classifiers [5, 8, 10]. In the freely accessible IBM quantum processors, the default number of measurements per job is set to 1024. While Refs. [8, 10] work close to these re-

strictions, Ref. [5] works with a much larger 50,000 measurements per kernel entry. Although the error mitigation technique used in [5] results in higher requirements for the number of measurements, 50,000 measurements is too large a number in practice for those without an exclusive access to a quantum computer. Ref. [10] uses 175 measurements to obtain the training kernel matrix and get good accuracies over the test set, but fails to mention the number of measurements used during the classification of a test datapoint. Ref. [8] uses the same number of measurements for both the training and the testing phases.

Our observations from FIG. 2 and the constraints of NISQ devices raise the following questions:

1. The number of measurements N needed to ensure accurate classification is dependent on the dataset and the choice of the kernel function. Can we derive a generic bound for N that would *reliably* reproduce the predictions of an ideal quantum kernel classifier?
2. Can we construct a reliable classifier which uses fewer N ?

We now answer both these questions in the affirmative.

V. RESULTS AND DISCUSSION

We here derive bounds over the number of measurements N which can ensure a small classification error, and perform numerical experiments showing the validity and usefulness of the bounds. Using methods from robust optimization, we then present a convex SVM program which is robust to the sampling noise by construction, and show its performance over different datasets.

Datasets. We present our results over three datasets: (1) Circles, (2) Two Moons, (3) Havlicek [5], generated over two qubits. All the figures in the main article correspond to the Circles dataset. All other details, e.g. the choice of quantum kernels and performance over an independent test set, are provided in Supp. Info. Our results in the main article are illustrated over the training data itself.

A. Bound on N from the accuracy of (SKC)

We derive here a bound for N which ensures, with high probability, that the stochastic kernel classifier (SKC) has a classification error smaller than the margin error of the exact kernel classifier (EKC).

Definition 7 (γ -margin violation error). *Given a dataset $\mathcal{D} \sim \mathcal{P}$, and a margin $\gamma \geq 0$, the set of points in \mathcal{D} which are γ -margin-misclassified by the classifier*

$f(\mathbf{x}) = f(\mathbf{x}|\beta, b; K)$ (6) is

$$\mathcal{S}_\gamma = \left\{ (\mathbf{x}_i, y_i) \in \mathcal{D} \mid y_i \left(\sum_{j=1}^m \beta_j K(\mathbf{x}_j, \mathbf{x}_i) + b \right) < \gamma \right\}. \quad (21)$$

The γ -margin violation error of the classifier f over the dataset \mathcal{D} is defined as

$$\epsilon_\gamma(f) = \frac{|\mathcal{S}_\gamma|}{|\mathcal{D}|}. \quad (22)$$

With $\gamma = 0$ in the above expression, the set \mathcal{S}_0 includes all the misclassifications made by the classifier over the dataset \mathcal{D} . Eq. (22) thus gives the *classification error*

$$\epsilon_0(f) = 1 - \text{Acc}(f) \quad (23)$$

of the classifier over dataset \mathcal{D} . On the other hand if $\gamma = 1$, the set \mathcal{S}_1 includes all those points (\mathbf{x}_i, y_i) which lie on the wrong side of the two margins $y_i \left(\sum_{j=1}^m \beta_j K(\mathbf{x}_j, \mathbf{x}_i) + b \right) = 1$. The fraction of such points in \mathcal{D} gives the *margin error* of the classifier. These are the points with nonzero contributions to the hinge loss term in (7).

The main result of this Section is that the classification error $\epsilon_0(f^{(N)})$ of the stochastic kernel classifier (SKC) can be guaranteed, with high probability, to be smaller than the γ -margin error $\epsilon_\gamma(f^*)$ of the true kernel classifier (EKC) when N is sufficiently large.

Theorem 2. Let $\mathcal{D} \sim \mathcal{P}$ denote a dataset of size $M = |\mathcal{D}|$. The classification error of the stochastic kernel classifier $f^{(N)}(\mathbf{x}) = f(\mathbf{x}|\beta^*, b^*; K^{(N)})$ (SKC) is bounded by the γ -margin error of the true classifier $f^*(\mathbf{x}) = f(\mathbf{x}|\beta^*, b^*; K^*)$ (EKC),

$$\epsilon_0(f^{(N)}) \leq \epsilon_\gamma(f^*), \quad (24)$$

with probability at least $(1 - \delta)$, whenever

$$N \geq \frac{c^2}{2\gamma^2} \|\beta^*\|^2 \log \frac{M}{\delta}. \quad (25)$$

The above theorem essentially extends the bound of Theorem 1 to any dataset of size M . We make an important remark regarding Theorem 2.

Remark 2. Given any dataset $\mathcal{D} \sim \mathcal{P}$ of size M , the number of measurements,

$$N = \frac{c^2}{2\gamma^2} m_{\text{sv}} C^2 \log \frac{M}{\delta}, \quad (26)$$

is sufficient to ensure that (24) holds with probability at least $1 - \delta$. Here m_{sv} is the number of support vectors in the training set, and C is the SVM regularization parameter (PRIMAL).

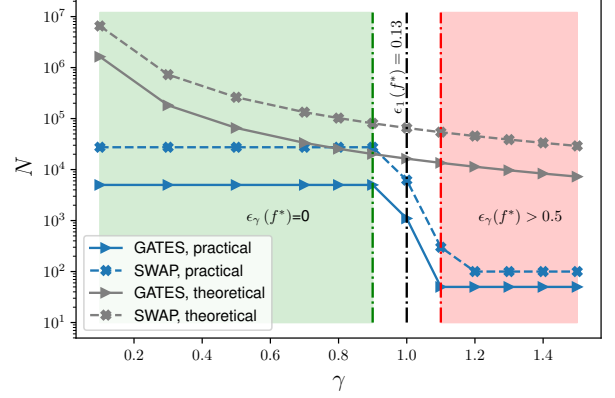


FIG. 3: Practical and theoretical bounds on N as a function of the margin γ for the Circles dataset. The green shading represents the region $\epsilon_\gamma(f^*) = 0$ where the stochastic kernel function (SKC) is expected to have perfect accuracy, with $\delta_{\text{target}} = 0.01$. The red shading represents the region with large margin error, $\epsilon_\gamma(f^*) > 0.5$, and low accuracy. The theoretical bound is smooth as a function of γ , but the practical bound shows a rapid change in N around $\gamma = 1$. The positions of the vertical green and red boundaries are expected to be problem dependent. The theoretical bound on N to obtain an accurate classifier (SKC) is optimal when we choose the largest γ in the green region.

Proof. The optimal primal and dual coefficients are related by $\beta_i^* = y_i \alpha_i^*$ [1]. Since $0 \leq \alpha_i \leq C$, we have $\|\beta^*\|^2 \leq m_{\text{sv}} C^2$, and the proof follows. \square

This result provides guidance for choosing the kernel function. A good choice of kernel K^* should classify accurately with a large margin γ , a small regularization parameter C , and few support vectors m_{sv} .

Definition 8 (Theoretical and practical bounds on N). Let the margin $\gamma \geq 0$ be specified for a dataset $\mathcal{D} \sim \mathcal{P}$ of size $M = |\mathcal{D}|$.

1. We define the theoretical bound from (25),

$$N_{\text{theory}} = \frac{c^2}{2\gamma^2} \|\beta^*\|^2 \log \frac{M}{\delta_{\text{target}}}, \quad (27)$$

where $\delta_{\text{target}} \ll 1$ is set to a small value.

2. We find the practical bound $N_{\text{practical}}$ by calculating the empirical probability of satisfying (24),

$$1 - \delta_{\text{emp}} = \frac{1}{N_{\text{trials}}} \sum_{s=1}^{N_{\text{trials}}} \mathbb{1}_{\epsilon_0(f^{(N)}\{s\}) \leq \epsilon_\gamma(f^*)}, \quad (28)$$

starting with some small N and increasing it until we obtain $\delta_{\text{emp}} < \delta_{\text{target}}$. An explicit algorithm is given in Appendix A.

Dataset	N needed for $\epsilon_0(f^{(N)}) = 0, \delta_{\text{target}} = 0.01$				$\epsilon_1(f^*)$
	GATES		SWAP		
	theory	practical	theory	practical	
Circles	2×10^4	$5 \times 10^3 \ddagger$	8×10^4	$2.7 \times 10^4 \ddagger$	0.133
Havlicek	330	110	1310	540	0.125
Two Moons	2×10^4	$2.5 \times 10^3 \ddagger$	7.8×10^4	$9.7 \times 10^3 \ddagger$	0.14

TABLE I: The number of measurements N needed to ensure that (SKC) reliably reproduces (EKC) over the training set itself, with probability of at least 99%. These numbers correspond to the green vertical line in Fig. 3. The practical bound on N is significantly smaller than the bound implied by Theorem 2. The GATES test requires an N which is about 4 times smaller than the SWAP test, as implied by Lemma 2. \ddagger indicates that N exceeds the IBMQ default value 1024.

We are interested in obtaining reliable reproduction of (EKC) from (SKC). Note that $\epsilon_0(f^*) = 0$ for all the datasets we have considered. Figure 3 shows the theoretical and practical bounds on N as a function of the margin γ for the Circles dataset. The green shading in it represents the region where $\epsilon_0(f^{(N)}) = 0$ is satisfied with $\delta_{\text{target}} = 0.01$. It thus leads to SKC which reliably reproduces EKC. In this region, the theoretical bound grows as $\gamma \rightarrow 0$ with an inverse quadratic dependence. The practical bound is insensitive to γ since it only depends on the value of the margin error and not the margin itself. The two bounds are closest to each other at the right edge of the region, and have been tabulated in TABLE I. We notice that the practical bound is about 3 – 5 times smaller, for a fixed circuit. This looseness of the theoretical bound is expected, since we used a subgaussian bound for the binomial distribution and not its complete information. The GATES circuit provides bounds (both theoretical and practical) which are about 4 times smaller than those for the SWAP circuit, consistent with Lemma 2.

Corollary 2.1. *Over a training set of size m , the empirical risk of (SKC)*

$$\epsilon_0(f^{(N)}) \leq \epsilon_1(f^*) \quad (29)$$

is bounded by the margin error of (EKC), with probability $1 - \delta$, whenever

$$N \geq \frac{c^2}{2} \|\beta^*\|^2 \log \frac{m}{\delta}. \quad (30)$$

The margin errors of (EKC) are listed in the right-most column of TABLE I. The corresponding mark is a black (dash-dotted) vertical line in FIG. 3. We stress that these values of N (at the black vertical line) are quite small compared to what is needed to ensure reliable reproduction of (EKC) (green region). The corollary above ensures a small empirical risk for (SKC).

Very importantly, the bound $N = \Omega(m_{\text{sv}} \log M)$, needed for reliably reproducing (EKC), is logarithmic in the size M of the dataset and linear in the number of support vectors m_{sv} of the training set. Often the number of support vectors is significantly smaller than the size m of the training set, $m_{\text{sv}} \ll m$ [9]. When applied over the training set itself, the number of circuit evaluations per kernel entry becomes $N = \Omega(\log m)$. Contrast this with the bound which can be derived to control the error in the training kernel matrix: demanding $\|\mathbf{K}^{(N)} - \mathbf{K}^*\| \leq \epsilon$ in the operator or Frobenius distance gives $N = \Omega(m^2/\epsilon^2)$ [5]. Indeed, the need to bring $\mathbf{K}^{(N)}$ close to \mathbf{K}^* , in addition to their error mitigation scheme, guided the choice of Ref. [5] of high $N = 50,000$ measurements per kernel entry. The entries for the Havlicek dataset in Table I are considerably lower, partly due to the logarithmic dependence on m .

We now address the second question: Can we construct a reliable classifier which uses fewer circuit evaluations?

B. Robust classifier for stochastic QEKs

The stochastic kernel classifier (SKC) $f^{(N)}(\mathbf{x}) = f(\mathbf{x}|\beta^*, b^*; K^{(N)})$ is constructed by solving (PRIMAL) for the optimal coefficients β^*, b^* over a training set given the exact training kernel matrix \mathbf{K}^* . The optimization problem over training data is a convex quadratic program since $\mathbf{K}^* \in \mathbb{S}_+^m$. In reality, the kernel matrix over a training dataset suffers from the same underlying noise which affects the classifier (SKC). If we measure the kernel matrix $\mathbf{K}^{(N)}$ with N measurements per kernel entry, the resulting optimization problem (PRIMAL) would generally not be convex. Such situations are encountered in optimization problems and can be handled by introducing a chance constraint [25, 26]. We show here how we may use the noise information (UM) of the training kernel matrix to construct more reliable classifiers.

An optimization problem with stochastic terms can be turned into a chance constraint problem as follows:

$$\begin{aligned} \min_{\beta \in \mathbb{R}^m, b, \tau \in \mathbb{R}} \quad & \tau \\ \text{s.t. Prob} \left(J(\beta, b; \mathbf{K}^{(N)}) \leq \tau \right) & \geq 1 - \delta, \end{aligned} \quad (31)$$

where $\delta \ll 1$ ensures that for most instantiations of the quantum kernel matrix $\mathbf{K}^{(N)}$, i.e. with high probability, the primal objective $J(\beta, b; \mathbf{K}^{(N)})$ is smaller than τ . This τ is the new objective which we wish to minimize. It is in fact a dummy variable that is the means to minimize the (stochastic) primal objective function with high probability.

The feasible set of a chance constraint is generally non-convex and makes the optimization problem intractable (although it is convex for some families of distributions [12]). The natural strategy in such cases is to construct convex approximations to the chance constraint [13, 27]. The chance constraint method (31) has been applied to

the dual SVM formulation by Bhadra et. al. [13], where convex approximations were derived for the chance constraint for a few different noise distributions. In the primal formulation (**PRIMAL**) considered in the present article, we note that there are two terms in the objective which are stochastic, namely, the hinge loss term and the regularization term given in the two lines of Eq. (7).

The hinge loss term penalizes margin errors in the training set. If a datapoint \mathbf{x}_i in the training set has a margin $\gamma_i \geq 1$, then it would not contribute to the hinge loss. If the regularization parameter C is set to a very large value, the hinge loss term essentially behaves as a constraint that ensures that no point in the training set has a margin violation. How can we minimize the hinge loss when dealing with a stochastic kernel matrix $\mathbf{K}^{(N)}$?

Lemma 3. *Let $\mathbf{x}_i \in \mathcal{D}_{\text{train}}$ and $\beta \in \mathbb{R}^m, b \in \mathbb{R}$. Datapoint \mathbf{x}_i would have zero hinge loss with probability at least $1 - \delta$,*

$$\text{Prob} \left(y_i \left(\sum_j \beta_j \mathbf{K}_{ij}^{(N)} + b \right) \geq 1 \right) \geq 1 - \delta, \quad (32)$$

if

$$y_i \left(\sum_j \beta_j \mathbf{K}_{ij}^* + b \right) \geq 1 + \frac{c}{2\sqrt{N}} \|\beta\| \kappa(\delta). \quad (33)$$

Proof. This is a direct application of Lemma 1, using the subgaussian norm from Lemma 2. \square

The SVM optimization, through the hinge loss term, finds coefficients β, b such that $1 - y_i \left(\sum_j \beta_j \mathbf{K}_{ij}^{(N)} + b \right)$ is minimized. The above Lemma suggests how we may minimize the hinge loss, when the kernel matrix is stochastic.

1. Given a stochastic kernel matrix $\mathbf{K}^{(N)}$ during training, Lemma 3 [Eq. (33)] provides a sufficient condition for the hinge loss contribution of \mathbf{x}_i to be minimized with probability $1 - \delta$. Importantly, Eq. (33) is convex in β, b and is cone representable.
2. The subgaussian bound (Lemma 1) for the quantum kernel distribution (Lemma 2) provides a very favorable scaling with δ and an inverse square root dependence with the number of measurements N .

The regularization term $\beta^\top \mathbf{K}^{(N)} \beta$ can be turned into a convex approximation directly by the use of an appropriate tailbound. The resulting chance constraint problem would thus be stated in terms of two parameters δ_1, δ_2 (see Supp. Info. III for a full derivation).

Theorem 3. *Let the kernel $\mathbf{K} = \mathbf{K}^{(N)} \in \mathbb{R}^m \times \mathbb{R}^m$ be inferred from N measurements per entry. The optimal primal objective $J^*(\mathbf{K}) := \min_{\beta, b} J(\beta, b; \mathbf{K})$ of (**PRIMAL**) is upper bounded by*

$$J^*(\mathbf{K}) \leq J_{\text{rob}}^*, \quad (34)$$

with probability at least $1 - \delta_1 - \delta_2$, where

$$J_{\text{rob}}^* = \min_{\beta \in \mathbb{R}^m, b \in \mathbb{R}} J_{\text{rob}}(\beta, b; \mathbf{K}^* | N, \delta_1, \delta_2) \quad (\text{ROB-PRIMAL})$$

is the optimal value of a Second-order Cone Program (SOCP), whose objective is given by

$$\begin{aligned} J_{\text{rob}}(\beta, b; \mathbf{K}^* | N, \delta_1, \delta_2) := \\ C \sum_{i=1}^m \max \left(1 + \frac{c}{2\sqrt{N}} \kappa \left(\frac{\delta_1}{m} \right) \|\beta\| - y_i \left(\sum_{j=1}^m \beta_j \mathbf{K}_{ij}^* + b \right), 0 \right) \\ + \frac{1}{2} \beta^\top \left(\mathbf{K}^* + \frac{c}{2\sqrt{N}} \kappa(\delta_2) \mathbf{I}_{m \times m} \right) \beta. \end{aligned} \quad (35)$$

Note that the objective (35) is very similar to the objective in (7) with two key differences:

1. The hinge-loss has an additional term whose origin is precisely the enforcement of $y_i \left(\sum_j \beta_j \mathbf{K}_{ij}^{(N)} + b \right) \geq 1$, with high probability as in Lemma 3, for all the m datapoints. Thus a condition against margin violation, which is *robust against stochasticity in the kernel matrix*, is built into the optimization problem itself (**ROB-PRIMAL**).
2. The kernel matrix in the regularization term is made larger by adding to its diagonal entries a term which arises precisely by requiring $\beta^\top \mathbf{K}^{(N)} \beta \leq \beta^\top \mathbf{K}^* \beta + t$ with probability $1 - \delta_2$ for some $t > 0$. The large deviation bound given by Lemma 1 implies that $t \geq \frac{c}{2\sqrt{N}} \|\beta\|^2 \kappa(\delta_2)$ is sufficient.

Suppose now that N is fixed to some preset value depending upon the constraints/budget of the user of a quantum processor. The points above suggest that a classifier constructed by solving (**ROB-PRIMAL**) would be more robust to the stochasticity of the training kernel matrix. We expect it to be a more reliable classifier at least over the training dataset. Moreover, since the kernel evaluations in a test dataset suffer from the same underlying noise (as the training kernel matrix), we expect it to be more reliable even over a test dataset (shown in Supp. Info.).

Definition 9. *The robust stochastic kernel classifier is*

$$h^{(N)}(\mathbf{x}) = f \left(\mathbf{x} | \beta_{\text{rob}}^*, b_{\text{rob}}^*; K^{(N)} \right), \quad (\text{RSKC})$$

where $\beta_{\text{rob}}^*, b_{\text{rob}}^*$ are solutions to the optimization problem (**ROB-PRIMAL**) for some fixed N , and $\delta_1, \delta_2 \ll 1$.

Definition 10. *The robust exact kernel classifier is*

$$h^*(\mathbf{x}) = f \left(\mathbf{x} | \beta_{\text{rob}}^*, b_{\text{rob}}^*; K^* \right), \quad (\text{REKC})$$

where $\beta_{\text{rob}}^*, b_{\text{rob}}^*$ are solutions to the optimization problem (**ROB-PRIMAL**). N , and $\delta_1, \delta_2 \ll 1$ are the same as in (**RSKC**).

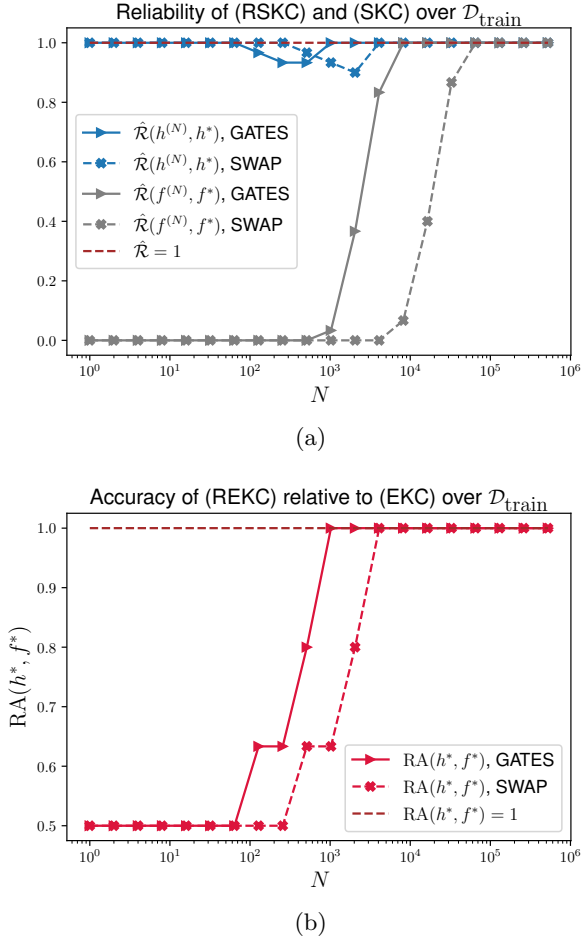


FIG. 4: (a) Comparison of the reliabilities of classifiers found using (PRIMAL) and the robust formulation (ROB-PRIMAL), for the Circles dataset. (b) The relative accuracy $RA(h^*, f^*)$ for the same dataset. Looking at (a) and (b) together, (i) the relative accuracy of h^* , and (ii) the reliability $\hat{\mathcal{R}}(h^{(N)}, h^*)$, become 1 much before the reliability $\hat{\mathcal{R}}(f^{(N)}, f^*)$ reaches 1.

Thus, we expect the reliability $\mathcal{R}(h^{(N)}, h^*)$ to be higher than $\mathcal{R}(f^{(N)}, f^*)$ for the same value of N and appropriately chosen small parameters δ_1, δ_2 . Note that the classifier h^* is dependent on N, δ_1, δ_2 via the optimization problem (ROB-PRIMAL), but it is *not stochastic*. (REKC) employs the exact kernel function K^* just as the true classifier (EKC). Fig. 4a shows $\hat{\mathcal{R}}(h^{(N)}, h^*)$ and $\hat{\mathcal{R}}(f^{(N)}, f^*)$, as functions of N for the Circles dataset: it is clear that the robust classifier $h^{(N)}$ reproduces h^* far more reliably than $f^{(N)}$ reproduces f^* , especially in the high noise regime (low N). In particular, $\hat{\mathcal{R}}(h^{(N)}, h^*) = 1$ even with a single measurement shot $N = 1$, but it comes at the cost of the accuracy of REKC.

Since our original aim was to implement the true classifier f^* with as few measurement shots per entry as possible, we define the relative accuracy of classifier h^* as

follows.

Definition 11 (Relative Accuracy). The relative accuracy of (REKC) with respect to (EKC) over any dataset is

$$RA(h^*, f^*) = \frac{Acc(h^*)}{Acc(f^*)}. \quad (36)$$

Reliability-Accuracy trade-off:

The classifier f^* has perfect accuracy over the training set in all the datasets considered here (for independent test set, see Supp. Info.). Fig. 4b shows the reliability $\hat{\mathcal{R}}(h^{(N)}, h^*)$ as well as the relative accuracy $RA(h^*, f^*)$, for the Circles dataset. For small N , the classifier h^* provides a low accuracy, but $h^{(N)}$ reproduces h^* perfectly. The low accuracy, for small N , can be understood from the expression for J_{rob} in Eq.(35); the data-independent terms containing δ_1, δ_2 dominate over the data-dependent terms containing \mathbf{K}^* , leading to fixed but inaccurate results.

With increasing N , increases in $RA(h^*, f^*)$ are accompanied by slight decreases in the reliability $\hat{\mathcal{R}}(h^{(N)}, h^*)$, constituting a trade-off between the two quantities. Finally, both these quantities reach their maximum value 1. The smallest value of N required to reliably agree with the results of (EKC) is tabulated in Table II, for both (SKC) and (RSKC). We note that the values of N , where the classifier $h^{(N)}$ reaches perfect reliability as well as perfect accuracy, are considerably smaller than those for the classifier $f^{(N)}$.

Note that (REKC) is the same as (EKC) in the limit of infinitely many measurements,

$$\lim_{N \rightarrow \infty} J_{\text{rob}}(\beta, b; \mathbf{K}^* | N, \delta_1, \delta_2) = J(\beta, b; \mathbf{K}^*). \quad (37)$$

However, we see from FIG. 4b and TABLE II that predictions of (RSKC) agree with (EKC) for significantly smaller values of N than what is needed for (SKC). The robust optimization program (ROB-PRIMAL) results in a classifier requiring only a fraction (ranging from $\frac{1}{16}$ to $\frac{1}{4}$) of the number of measurements N to reliably implement the true classifier (EKC). We thus recommend using the robust optimization problem (ROB-PRIMAL) in place of the standard SVM optimization (PRIMAL).

(ROB-PRIMAL) is second-order cone representable (details in Supp. Info. III), and several efficient algorithms have been developed for such optimization problems [28]. SOCP have found applications in many engineering areas such as filter design, truss design and grasping force optimization in robotics (see Ref. [28] for a survey of applications). SOCP has also been very useful for many machine learning applications e.g. robust classification under uncertainty [13, 29, 30].

VI. SUMMARY AND OUTLOOK

We have studied the role of N , the number of measurements used to evaluate a quantum kernel, for a classifica-

Dataset	N needed for perfect reliability with (EKC)			
	GATES		SWAP	
	SKC	RSKC	SKC	RSKC
Circles	$2^{13} \ddagger$	2^{10}	$2^{16} \ddagger$	$2^{12} \ddagger$
Havlicek [5]	2^7	2^5	2^9	2^7
Two Moons	2^9	2^8	$2^{12} \ddagger$	2^{10}

TABLE II: The number of measurements N at which perfect reliability^a with respect to (EKC) is achieved over the training dataset for classifiers (SKC) and (RSKC). The instantiations of the kernel function $K^{(N)}$ are the same for both. The robust classifier reduces the number of circuit evaluations needed (per kernel entry) by a factor of 4 to 16. \ddagger denotes that N exceeds the IBMQ default value 1024.

^a The values for (SKC) in this table turn out the same as the corresponding entries for $N_{\text{practical}}$ in TABLE I, expressed in exponential notation $N = 2^n$, $n = \lceil \log_2(N_{\text{practical}}) \rceil$.

tion task. Our considerations have focused on providing the same predictions as the ideal quantum kernel classifier ($N \rightarrow \infty$), *not* to closely approximate the kernel function itself. We noted that the classification accuracy is a poor performance metric in the presence of noise, and defined an empirical reliability that meaningfully captures the effects of noise. The circuit used to evaluate the quantum kernel plays an important role in the analysis, and we have shown that the GATES test is preferable to the SWAP test for any N (Lemma 2). We introduced a generic uncertainty model (UM) that can handle any source of noise. Our results in the article have considered only the fundamental sampling noise; the modification to the uncertainty model in presence of other noise sources is given in the Supp. Info.

Our analysis assumed that we have access to the exact kernel matrix $\mathbf{K}^* \in \mathbb{S}_+^m$ over the training dataset of size m . We then showed that $N = \Omega(\log m)$ measurements are needed for reliable reproduction of the ideal quantum classifier over the training dataset. This is in contrast to the requirement that $N = \Omega(m^2/\epsilon^2)$, when one evaluates

$\|\mathbf{K}^{(N)} - \mathbf{K}^*\| \leq \epsilon$ up to a precision of ϵ . Physically, this arises from the fact that in an SVM the boundary (and not the bulk) carries the information relevant to the classifier.

Our main contributions are the following. We developed a bound on N (Theorem 1), which ensures that a datapoint is reliably (i.e. with high probability) classified the same way as an ideal quantum kernel classifier would do. We then extended the result to any dataset of M points (Theorem 2), deriving a bound on N which ensures that the classification error is smaller than the margin error of the ideal classifier. We also computed a practical bound (Definition 8) on N which ensures high empirical reliability. We then investigated whether it was possible to reduce N further, while still reliably reproducing the ideal classifier. We used the chance constraint approach to the original SVM (robust formulation) and showed that it is indeed possible to substantially reduce N .

Finally, we point out some open questions related to our results that are worth exploring, especially in light of the limitations of near-term quantum hardware.

1. To optimize N for an accurate stochastic classifier (SKC), we need to maximize γ while maintaining low γ -margin errors of the exact classifier (EKC), i.e. stay just left of the vertical green line in FIG. 3. Such a value of γ would be problem dependent, but can we develop a criterion to identify it?
2. To optimize N for a robust stochastic classifier (RSKC) while ensuring high relative accuracy, we need to estimate where RA reaches 1 in FIG. 4b. Such an N would also be problem dependent, but can we find a method to identify it?
3. In practice, we may only have access to approximate $\mathbf{K}^{(N)}$ over the training data, instead of the exact \mathbf{K}^* . Such a $\mathbf{K}^{(N)}$ may not be positive, and modifications [8, 10] would be needed to make it positive for the construction of the SVM classifier. How sensitive would the optimal parameters β, b of the SVM be, as a function of N ?

[1] B. Scholkopf and A. J. Smola, *Learning with Kernels: Support Vector Machines, Regularization, Optimization, and Beyond* (MIT Press, Cambridge, MA, USA, 2001).
[2] M. Schuld and N. Killoran, *Phys. Rev. Lett.* **122**, 040504 (2019).
[3] M. Schuld, (2021), [arXiv:2101.11020 \[quant-ph\]](https://arxiv.org/abs/2101.11020).
[4] J. Kübler, S. Buchholz, and B. Schölkopf, *Advances in Neural Information Processing Systems* **34** (2021).
[5] V. Havlíček, A. D. Córcoles, K. Temme, A. W. Harrow, A. Kandala, J. M. Chow, and J. M. Gambetta, *Nature* **567**, 209 (2019).
[6] Y. Liu, S. Arunachalam, and K. Temme, *Nature Physics*

17, 1013 (2021).
[7] H.-Y. Huang, M. Broughton, M. Mohseni, R. Babbush, S. Boixo, H. Neven, and J. R. McClean, *Nature Communications* **12**, 2631 (2021).
[8] X. Wang, Y. Du, Y. Luo, and D. Tao, *Quantum* **5**, 531 (2021).
[9] I. Steinwart, *Advances in Neural Information Processing Systems* **16** (2003).
[10] T. Hubregtsen, D. Wierichs, E. Gil-Fuster, P.-J. H. S. Derks, P. K. Faehrmann, and J. J. Meyer, (2021), [arXiv:2105.02276 \[quant-ph\]](https://arxiv.org/abs/2105.02276).
[11] C. Blank, D. K. Park, J.-K. K. Rhee, and F. Petruccione,

npj Quantum Information **6**, 41 (2020).

[12] A. Prékopa, *Stochastic Programming* (Kluwer Academic Publishers, Dordrecht, The Netherlands, 1995).

[13] S. Bhadra, S. Bhattacharya, C. Bhattacharyya, and A. Ben-Tal, Proceedings of the 27th International Conference on Machine Learning (2010).

[14] K. Bharti, A. Cervera-Lierta, T. H. Kyaw, T. Haug, S. Alperin-Lea, A. Anand, M. Degroote, H. Heimonen, J. S. Kottmann, T. Menke, W.-K. Mok, S. Sim, L.-C. Kwek, and A. Aspuru-Guzik, *Rev. Mod. Phys.* **94**, 015004 (2022).

[15] J. M. Kübler, A. Arrasmith, L. Cincio, and P. J. Coles, *Quantum* **4**, 263 (2020).

[16] A. Arrasmith, L. Cincio, R. D. Somma, and P. J. Coles, *Operator sampling for shot-frugal optimization in variational algorithms* (2020).

[17] A. Gu, A. Lowe, P. A. Dub, P. J. Coles, and A. Arrasmith, *Adaptive shot allocation for fast convergence in variational quantum algorithms* (2021).

[18] V. V. Buldygin and Y. V. Kozachenko, *Ukrainian Mathematical Journal* **32**, 483.

[19] J. Cervantes, F. Garcia-Lamont, L. Rodríguez-Mazahua, and A. Lopez, *Neurocomputing* **408**, 189 (2020).

[20] V. N. Vapnik, *Statistical Learning Theory* (Wiley, New York, 1998).

[21] S. Lloyd, M. Schuld, A. Ijaz, J. Izaac, and N. Killoran, (2020), [arXiv:2001.03622 \[quant-ph\]](https://arxiv.org/abs/2001.03622).

[22] M. A. Nielsen and I. L. Chuang, *Quantum Computation and Quantum Information: 10th Anniversary Edition*, 10th ed. (Cambridge University Press, USA, 2011).

[23] P. Massart, *Concentration Inequalities and Model Selection*, edited by J. Picard (Springer Berlin Heidelberg, 2007).

[24] N. A. Nghiem, S. Y.-C. Chen, and T.-C. Wei, *Phys. Rev. Research* **3**, 033056 (2021).

[25] A. Charnes, W. W. Cooper, and G. H. Symonds, *Management Science* **4**, 235 (1958).

[26] A. Prékopa, On probabilistic constrained programming, in *Proceedings of the Princeton Symposium on Mathematical Programming* (Princeton University Press, 1970) pp. 113–138.

[27] A. Nemirovski and A. Shapiro, *SIAM Journal on Optimization* **17**, 969 (2007), <https://doi.org/10.1137/050622328>.

[28] M. S. Lobo, L. Vandenberghe, S. Boyd, and H. Lebet, *Linear Algebra and its Applications* **284**, 193 (1998), international Linear Algebra Society (ILAS) Symposium on Fast Algorithms for Control, Signals and Image Processing.

[29] G. R. Lanckriet, L. E. Ghaoui, C. Bhattacharyya, and M. I. Jordan, *J. Mach. Learn. Res.* **3**, 555–582 (2003).

[30] A. Ben-Tal, S. Bhadra, C. Bhattacharyya, and J. Saketha Nath, *Mathematical Programming* **127**, 145 (2011).

[31] V. Bergholm, J. Izaac, M. Schuld, C. Gogolin, M. S. Alam, S. Ahmed, J. M. Arrazola, C. Blank, A. Delgado, S. Jahangiri, K. McKiernan, J. J. Meyer, Z. Niu, A. Száva, and N. Killoran, *Pennylane: Automatic differentiation of hybrid quantum-classical computations* (2018).

[32] L. A. Goldberg and H. Guo, *computational complexity* **26**, 765 (2017).

[33] V. V. Buldigin and K. K. Moskvichova, *Teor. Ĭmovir. Mat. Stat.* , 28 (2011).

[34] J. Arbel, O. Marchal, and H. D. Nguyen, On strict sub-gaussianity, optimal proxy variance and symmetry for bounded random variables (2019), [arXiv:1901.09188 \[math.PR\]](https://arxiv.org/abs/1901.09188).

[35] G. Boole, *The Mathematical Analysis of Logic: Being an Essay Towards a Calculus of Deductive Reasoning*, Cambridge Library Collection - Mathematics (Cambridge University Press, 2009).

Appendix A: Computing the number of measurements needed for kernel evaluation

We follow the algorithm below to compute the practical bound on N , from the Definition 8. Fig. 3 shows that this practical bound on N is always below the theoretical bound given by Theorem 2.

Algorithm 1 Computing $N_{\text{practical}}$

Require: \mathcal{D} , K^* , γ
 /* Given: β^* , b^* over training data $\mathcal{D}_{\text{train}}$ */
 Initialize N_{start} , N_{step} , $\delta_{\text{target}} = 0.01$, $N_{\text{trials}} = 200$
for $i \leftarrow 1$ to $|\mathcal{D}|$ **do**
 for $j \leftarrow 1$ to $|\mathcal{D}_{\text{train}}|$ **do**
 $\mathbf{K}[i, j] \leftarrow K^*(\mathbf{x}_i, \mathbf{x}_j)$
 /* Above K_{ij}^* needed for computation of $f^*(\mathbf{x}_i)$ */
 $\epsilon_\gamma \leftarrow \sum_{i \in [|\mathcal{D}|]} \mathbb{1}_{y_i f^*(\mathbf{x}_i) < \gamma}$
 $N \leftarrow N_{\text{start}}$
while $\delta_{\text{emp}} \geq \delta_{\text{target}}$ **do**
 $N \leftarrow N + N_{\text{step}}$
 for $t \leftarrow 1$ to N_{trials} **do**
 $c \leftarrow 0$
 for $i \leftarrow 1$ to $|\mathcal{D}|$ **do**
 for $j \leftarrow 1$ to $|\mathcal{D}_{\text{train}}|$ **do**
 $\mathbf{K}[i, j] \leftarrow K^{(N)}\{t\}(\mathbf{x}_i, \mathbf{x}_j)$
 /* $K^{(N)}\{t\}(\mathbf{x}_i, \mathbf{x}_j)$ for computing $f^{(N)}\{t\}(\mathbf{x}_i)$ */
 $\epsilon_0 \leftarrow \sum_{i \in [|\mathcal{D}|]} \mathbb{1}_{y_i f^{(N)}\{t\}(\mathbf{x}_i) < 0}$
 if $\epsilon_0 > \epsilon_\gamma$ **then**
 $c \leftarrow c + 1$
 $\delta_{\text{emp}} \leftarrow c / N_{\text{trials}}$
return N

Supplementary Information

Reliable quantum kernel classification using fewer circuit evaluations

I. DATASETS AND KERNEL EMBEDDING CHOICES

Datasets. Our simulations with quantum kernels are performed using the PennyLane python package developed by Xanadu [31]. We use three datasets to illustrate our results: `make_circles` (Circles) and `make_moons` (Moons) dataset from `sklearn` and the Havlicek generated dataset. The latter is generated by using `IQPEmbedding` and following the procedure outlined in ref. [5]. We then use the same embedding kernel to classify the generated dataset. Our choice of kernel functions for the other two datasets (Circles and Moons) are based on a trial and error process where we tried different embedding kernels and chose the one that returned the highest test accuracies. Our choice of the kernel function for the dataset Circles is the simple `AngleEmbedding` circuit shown in fig. (S1) in the main article. The Moons dataset was found to give very high test accuracies by using a X-rotation (`AngleEmbedding`) after the application of the `IQPEmbedding`. All of these kernels are defined over 2-qubits (all datasets here are 2-dimensional) with no repeating layers and no tunable circuit parameters. We have chosen a smaller number of training samples, keeping in view the restrictions placed by near-term devices [8].

TABLE S1 shows training and test sizes. For the Havlicek dataset we use $m = 40$ (20 labels per class as used in ref. [5]), and a equal test size $M = 40$, exactly as used in their study. All the training and test datasets used here are balanced. These kernel choices were used in the main article and all of them lead to nearly perfect test accuracies for the exact kernel classifier (`EKC`).

Quantum Kernel embeddings.

It is easy to see that the kernel function is equivalent to an inner product in the *feature* Hilbert space $\mathcal{H} \otimes \mathcal{H}^*$ since, for every pair $|\phi(\mathbf{x}_i)\rangle, |\phi(\mathbf{x}_j)\rangle \in \mathcal{H}$, we have $|\phi(\mathbf{x}_i)\rangle \otimes |\phi^*(\mathbf{x}_i)\rangle, |\phi(\mathbf{x}_j)\rangle \otimes |\phi^*(\mathbf{x}_j)\rangle \in \mathcal{H} \otimes \mathcal{H}$, whose inner product is the quantum kernel $K(\mathbf{x}_i, \mathbf{x}_j) = |\langle \phi(\mathbf{x}_i) | \phi(\mathbf{x}_j) \rangle|^2$. One can express this in terms of an outer product $|\phi(\mathbf{x}_j)\rangle \otimes \langle \phi(\mathbf{x}_j) | \in \mathcal{H} \otimes \mathcal{H}^*$ where the embedding vectors are density matrices and the kernel can be described via the Hilbert-Schmidt inner product as given in (8).

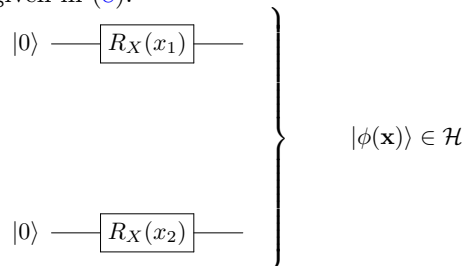


FIG. S1: **Example: Angle Embedding.** A simple quantum embedding circuit which is embedding the input vector $\mathbf{x} = (x_1, x_2) \in \mathbb{R}^2$ into a quantum state $|\phi(\mathbf{x})\rangle$ in the 2-qubit Hilbert space \mathcal{H} , by applying a rotation along the X-axis by angle x_i over the corresponding qubit starting in the state $|0\rangle$. The transition probability between two such quantum states $K(\mathbf{x}, \mathbf{x}') = |\langle \phi(\mathbf{x}') | \phi(\mathbf{x}) \rangle|^2$ is a valid kernel function and is known as a Quantum Embedding Kernel (QEK).

Note that the `AngleEmbedding` shown in fig. S1 is a simple quantum embedding circuit which can in fact be simulated efficiently on a classical machine [5, 32]. However, our study does not directly concern the debate regarding quantum advantage. Rather, our focus is on the number of measurements N needed to reliably implement a quantum kernel classifier.

All the figures presented in the main article used the Circles dataset with the `AngleEmbedding` kernel.

Change of kernel embedding. Our results derived in the main article over the bounds on N as well as the improved performance of the robust classifiers hold regardless of the choice of kernel. We illustrate this using Moons dataset with the `IQPEmbedding` which does not classify the test set with as high accuracy as when used in conjunction with a X-rotation (`AngleEmbedding`). The training and test sets are held the same. The accuracy over the test set for the true classifier (`EKC`) in this case is 88.3%, as opposed to 99.72% for the kernel choice in TABLES1. FIG. S2c shows that the reliabilities of the robust classifiers are far higher for both the kernel choices. The top panel shows the performance of the original kernel choice and the bottom panel shows the performance of the `IQPEmbedding` alone over the same test set.

Dataset	Kernel Embedding	Training size m	Test size M	Test Accuracy
Havlicek [5]	IQPEmbedding	40	40	100%
Circles (make_circles)	AngleEmbedding	30	370	100%
Moons (make_moons)	IQPEmbedding + AngleEmbedding	40	360	99.7%

TABLE S1: Summary of datasets and quantum kernel embedding choices. The Moons dataset is encoded using the IQPEmbedding followed by a X-rotation by an angle given by the corresponding values of the feature vector. All embedding circuits are defined over 2 qubits with no layer repetitions and no tunable parameters. These choices lead to very high test accuracy for the true kernel classifier (EKC).

Dataset	N needed for perfect reliability with (EKC)			
	GATES		SWAP	
	SKC	RSKC	SKC	RSKC
Circles	$2^{14} \ddagger$	2^{10}	$2^{16} \ddagger$	$2^{12} \ddagger$
Havlicek [5]	2^9	2^6	$2^{11} \ddagger$	2^8
Two Moons	2^{13}	2^9	$2^{15} \ddagger$	$2^{11} \ddagger$

TABLE S2: N at which perfect reliability, with respect to f^* , is achieved over the test dataset for classifiers (SKC) and (RSKC). Training test is the same as considered in the main article. The instantiations of the kernel function $K^{(N)}$ are the same for both. The Robust classifier reduces the number of circuit evaluations needed (per kernel evaluation) by a factor of 4 to 16 in the datasets considered here. \ddagger denotes N exceeding IBM default value of 1024. The Moons dataset needs very large N to reach “perfect” reliability with (EKC). For this case, we report N for which it achieves $> 98\%$ reliability with (EKC). See FIG. S2a and S2b.

We see that the choice of kernel has made the N much higher than if we had used the IQPEmbedding along with the X-rotation (as done in the main article). The classifier (SKC) requires far more circuit evaluations to ensure a reliability close to one. Bad kernel choices may thus result in very large overheads for N . However, the advantages of the robust classifiers are still valid.

Total circuit evaluations. We have so far discussed the reduction in the number of circuit evaluations per kernel entry. TABLE S2 shows the N needed per kernel entry. However, we note that the number of support vectors increase when one solves the robust optimization problem (ROB-PRIMAL). If the size of the test set is M , we need $m_{sv}M$ total circuit evaluations where m_{sv} is the number of support vectors. However, an advantage is still maintained by the robust classifier in terms of the total number of measurements needed. For the circles and moons dataset, we still find a $> 75\%$ reduction in the total circuit evaluations and $> 50\%$ for the Havlicek dataset.

Other sources of noise. Recently, kernel estimates have been introduced that correct for depolarizing error as well [10]. These estimates are not unbiased, i.e. $\mathbb{E}[K^{(N)}(\mathbf{x}_i, \mathbf{x}_j)] \neq K^*(\mathbf{x}_i, \mathbf{x}_j)$, and requires separate treatment. In such a case, we may write the final kernel function K_{ij} as

$$K_{ij} = \hat{K}_{ij} + \Delta K_{ij}^{(N)} + \Delta K_{ij}^{(\text{other})}, \quad (\text{S1})$$

where $\mathbb{E}[K_{ij}] = \hat{K}_{ij} \neq K_{ij}^*$ which must be estimated using a bias-correcting procedure (such as the one for depolarizing noise in ref. [10]). All other noise contributions have been subsumed into $\Delta K_{ij}^{(\text{other})}$ whose expectation value is taken as zero without loss of generality. Assuming they are independent sources of noise, we would have

$$\sigma_0^2 = \sigma^2(K_{ij}) = \frac{c^2}{4N} + \sigma^2(\text{other}), \quad (\text{S2})$$

and the methods we develop in the article can be applied with the above σ_0 in the uncertainty model UM. However, if the noise biases the kernel value, we would need to compare all our results to \hat{K} instead of K^* . All our results in this article were in the presence of the sampling noise alone to clarify its contribution.

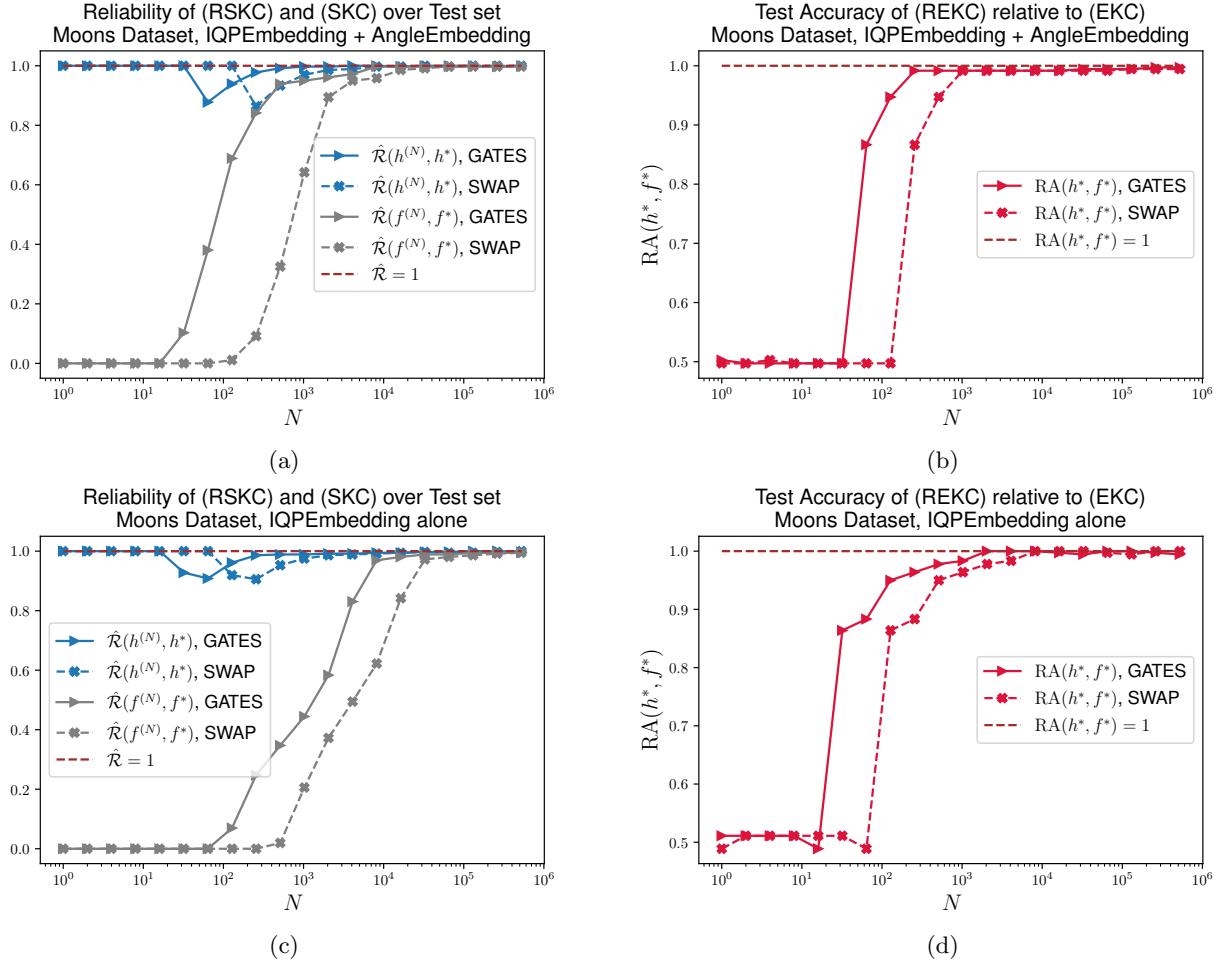


FIG. S2: The test accuracy of the true classifier (EKC) over the same test set is 88.3% when we use the kernel choice is IQPEmbedding alone (bottom panel) for the Moons dataset and is 99.7% when the embedding circuit has an additional X-rotation (top panel). The N requirement for (SKC) has gone up in the bottom panel. However, the robust classifier still provides a large advantage: It can provide very high reliability and reproduce (EKC) for much smaller N .

II. SUBGAUSSIAN PROPERTY OF BERNOULLI RANDOM VARIABLES

A random variable ξ (centered, $\mathbb{E}\xi = 0$) is called subgaussian if there exists $a \in [0, \infty)$ such that

$$\mathbb{E}e^{\lambda\xi} \leq e^{\frac{a^2\lambda^2}{2}}, \quad \forall \lambda \in \mathbb{R} \quad (\text{S1})$$

and the smallest such a

$$\sigma(\xi) = \inf \{a \geq 0 \mid \mathbb{E}\exp\{\lambda\xi\} \leq \exp\{a^2\lambda^2/2\}, \quad \forall \lambda \in \mathbb{R}\} \quad (\text{S2})$$

is called the *subgaussian norm* of ξ (smallest such $a^2 = \sigma^2(\xi)$ has been called the optimal variance proxy). We note two straight-forward properties of the subgaussian norm [33]: (1) *Scaling*, i.e. $\sigma^2(\lambda X) = \lambda^2\sigma^2(X)$ for any $\lambda \in \mathbb{R}$, and (2) *Sub-additivity*, i.e. for any independent X_k , $k = \{1, 2, \dots, N\}$, $\sigma^2(\sum_{k=1}^N X_k) \leq \sum_{k=1}^N \sigma^2(X_k)$. Equality holds for independent and identical random variables ξ_k , $k = \{1, 2, \dots, N\}$, $\sigma^2(\sum_{k=1}^N \xi_k) = N\sigma^2(\xi_1)$.

For both GATES and SWAP, the mean of the estimated kernel matches the true kernel $\mathbb{E}[K_N(\mathbf{x}_i, \mathbf{x}_j)] = K^*(\mathbf{x}_i, \mathbf{x}_j)$. The variances of these two estimates are given by

$$\text{Var}(K_N(\mathbf{x}_i, \mathbf{x}_j)) = \begin{cases} \frac{K_{ij}^*(1-K_{ij}^*)}{N} & (\text{GATES}) \\ \frac{(1-(K_{ij}^*)^2)}{N} & (\text{SWAP}). \end{cases} \quad (\text{S3})$$

In Eq. (S3) since $0 \leq K_{ij}^* \leq 1$, we have $K_{ij}^*(1 - K_{ij}^*) \leq 1 - (K_{ij}^*)^2$, implying a lower variance for the GATES circuit for the same N . Thus the SWAP circuit is affected more by the sampling noise. The maximum value of $K_{ij}^*(1 - K_{ij}^*)$ is 0.25 whereas $1 - (K_{ij}^*)^2$ can take a maximum value of 1. This bounds the variance of $K_{ij}^{(N)}$ in Eq. (S3) (equivalently the variance of $\Delta K_{ij}^{(N)}$).

We note that the distributions given by (GATES) and (SWAP) are subgaussian. Furthermore, we note that $\Delta K_{ij}^{(N)}$ in (9) can be expressed as the sum of N i.i.d. centered Bernoulli random variables $X_k(p) \sim B^{(0)}(1, p) = p - B(1, p)$, $k = \{1, 2, \dots, N\}$ for both the GATES and the SWAP tests

$$N\Delta K_{ij}^{(N)} = \begin{cases} \sum_{k=1}^N X_k(p), & p = K_{ij}^* & \text{(GATES)} \\ 2\sum_{k=1}^N X_k(p), & p = \frac{1+K_{ij}^*}{2} & \text{(SWAP)}. \end{cases} \quad (\text{S4})$$

Stated another way, the prefactor of 2 above for the SWAP test would have the effect of increasing its variance and thus makes it less reliable for the same number of measurements N . Bernoulli random variables are subgaussian [33, 34] and their properties are covered in section II. We use these properties to derive tail bounds over the kernel distributions.

We omit the random variable $\xi \sim B^{(0)}(1, p)$ while denoting the subgaussian norm for a centered Bernoulli distribution and simply write $\sigma(p)$. The optimal variance proxy for a centered Bernoulli distribution was derived in [33] and is given by ($q = 1 - p$)

$$\sigma^2(p) = \begin{cases} 0 & p = \{0, 1\} \\ 0.25 & p = 0.5 \\ \frac{p-q}{2(\ln(p)-\ln(q))} & \text{otherwise.} \end{cases} \quad (\text{S5})$$

Its properties were derived in lemma 2.1 of [33] from which we note that $\sigma^2(p)$ is monotonically increasing for $p \in (0, 1/2)$ and monotonically decreasing for $p \in (1/2, 1)$. It is also symmetrical $\sigma^2(p) = \sigma^2(q)$ (where $q = 1 - p$). It takes on its maximum value of $1/4$ when $p = q = 1/2$. Using the maximum value of the subgaussian norm for Bernoulli random variables above and eq. (S4) for the two different circuits gives us the bound used in (14).

III. CHANCE CONSTRAINT PROGRAMMING FOR (PRIMAL)

We shall assume below that the kernel matrix $\mathbf{K} = \mathbf{K}^{(N)} = \mathbf{K}^* - \Delta\mathbf{K}^{(N)}$ is stochastic and entries of $\Delta\mathbf{K}^{(N)}$ satisfy the uncertainty model (UM) with the bound given by Eq. (14).

The hinge loss given by

$$L(\beta, b; \mathbf{K}) = \sum_{i=1}^m \max\left(1 - y_i\left(\sum_j \mathbf{K}_{ij}\beta_j + b\right), 0\right) \quad (\text{S1})$$

is also subject to the stochasticity of the kernel matrix \mathbf{K} . Whether the term is zero or positive depends on the particular instantiation of the kernel matrix. This will have to be handled by a chance constraint approach. The same objective in the SVM primal problem (7) can be written as

$$\min_{t, \xi, \beta, b} J(t, \xi, \beta, b; \mathbf{K}) := C \sum_{i=1}^m \xi_i + t, \quad (\text{PRIMAL-2})$$

with the hinge-loss term as the two constraints

$$\mathbb{I}\mathbf{E}_i : \xi_i \geq 1 - y_i\left(\sum_{j=1}^m \mathbf{K}_{ij}\beta_j + b\right), \quad (\text{constraint-1})$$

and

$$\xi_i \geq 0, \quad i \in [m]. \quad (\text{S2})$$

The quadratic term is translated to the constraint

$$\frac{1}{2}\beta^\top \mathbf{K}\beta \leq t. \quad (\text{constraint-2})$$

The constraints ([constraint-1](#)) and ([constraint-2](#)) are dependent on the particular instantiation of the stochastic kernel matrix \mathbf{K}_N and we thus advocate the strategy of satisfying them with high probability. We denote the probability of violation of *any* one constraint IE_i in ([constraint-1](#)) by $\delta_1 \ll 1$ and the probability of violating the constraint ([constraint-2](#)) by $\delta_2 \ll 1$. The intersection of all the inequalities IE_i is satisfied with a high probability $1 - \delta_1$, which gives us a sufficient condition that each inequality be satisfied with the higher probability of $1 - \delta_1/m$ (union bound [III A](#))

$$\text{Prob}\left(\xi_i \geq 1 - y_i\left(\sum_j \mathbf{K}_{ij}\beta_j + b\right)\right) \geq 1 - \frac{\delta_1}{m}, \quad (\text{chance-1})$$

and

$$\text{Prob}\left(\frac{1}{2}\beta^\top \mathbf{K} \beta \leq t\right) \geq 1 - \delta_2. \quad (\text{chance-2})$$

We derive sufficient conditions for the constraints ([chance-1](#)) and ([chance-2](#)) below which lead to theorem [3](#). At optimality, we shall denote $J(t, \xi, \beta, b; \mathbf{K}) = J^*(\mathbf{K})$, dropping the optimal variables t^*, ξ^*, β^*, b^* from the notation.

A. Chance constraint: Union bound

When multiple chance constraints are present, we have invoked the well-known union bound to derive our results [\[35\]](#). Suppose the chance constraints to be satisfied are some inequalities A_i , $i \in [m]$, we denote its conjugate as \bar{A}_i which is the violation of inequality A_i . We would like all the constraints A_i , i.e. $\cap_i^m A_i$, to be satisfied and derive a sufficient condition for it. Since $\overline{\cap_i^m A_i} = \cup_i \bar{A}_i$, we consider the probability of the union of all constraint violations

$$\begin{aligned} \text{Prob}(\bar{A}_1 \cup \bar{A}_2 \cup \dots \bar{A}_m) &\leq \sum_{i=1}^m \text{Prob}(\bar{A}_i), \\ &\leq \delta, \end{aligned} \quad (\text{S3})$$

for some small parameter $0 < \delta \ll 1$. This provides the sufficient condition

$$\begin{aligned} \text{Prob}(\bar{A}_i) &\leq \frac{\delta}{m}, \\ \text{Prob}(A_i) &\geq 1 - \frac{\delta}{m}. \end{aligned} \quad (\text{S4})$$

B. Proofs

Theorem [2](#) follows a procedure similar to that of theorem [1](#) but additionally uses the Union bound mentioned above. We provide a detailed proof of theorem [3](#) below. The proof follows a similar procedure as that for theorem [2](#) and is detailed here for clarity.

Proof of Theorem 3. The optimization problem ([PRIMAL-2](#)) subject to the chance constraints ([chance-1](#)) and ([chance-2](#)) is in general nonconvex and we now derive sufficient conditions for the chance constraints ([chance-1](#)) and ([chance-2](#)) using the uncertainty model \mathcal{P}_N . We first write the random kernel K as the sum of its expected and stochastic parts $K_{ij} = K_{ij}^* - \Delta K_{ij}^{(N)}$ in the chance constraint ([chance-1](#))

$$P\left(y_i \sum_j \beta_j \Delta K_{ij}^{(N)} \leq h\right) \geq 1 - \frac{\delta_1}{m}, \quad (\text{S5})$$

where $h = y_i(\sum_j K_{ij}^* \beta_j + b) + \xi_i - 1$. We derive a tail bound for the constraint violation probability for the random variable $X = y_i \sum_j \beta_j \Delta K_{ij}^{(N)}$ using lemma [1](#) and find the sufficient condition

$$\xi_i \geq 1 - y_i\left(\sum_j K_{ij}^* \beta_j + b\right) + \frac{c}{2\sqrt{N}} \kappa\left(\frac{\delta_1}{m}\right) \|\beta\|, \quad (\text{S6})$$

for satisfying the chance constraint (chance-1).

We similarly derive a sufficient condition for the chance constraint (chance-2). With the kernel matrix $\mathbf{K}_{ij} = \mathbf{K}_{ij}^* - \Delta\mathbf{K}_{ij}^{(N)}$, we define the random variable

$$R = -\frac{1}{2}\beta^\top \Delta\mathbf{K}_N \beta = -\frac{1}{2} \sum_{ij} \Delta K_{ij}^{(N)} \beta_i \beta_j. \quad (\text{S7})$$

We rewrite (chance-2) as $P(R \leq t') \leq \delta_2$ and apply lemma 1 to find the sufficient condition. We detail it below for clarity:

$$\begin{aligned} t' &\geq \frac{c}{4\sqrt{N}} \|\beta\|^2 \kappa(\delta_2) \\ t &\geq \frac{1}{2}\beta^\top \mathbf{K}^* \beta + \frac{c}{4\sqrt{N}} \|\beta\|^2 \kappa(\delta_2) \\ &= \frac{1}{2}\beta^\top \left(\mathbf{K}^* + \frac{c}{2\sqrt{N}} \kappa(\delta_2) I \right) \beta \end{aligned} \quad (\text{S8})$$

for satisfying the chance constraint (chance-2).

Use sufficient conditions (S6), (S8) for the objective (PRIMAL-2) and eliminate (dummy) variable t . Apply the union bound (III A) for conditions (chance-1) and (chance-2) to show $\forall \beta, b$:

$$\text{Prob}(J(\beta, b; \mathbf{K}) \leq J_{\text{rob}}(\xi, \beta, b; \mathbf{K}^*)) \geq 1 - \delta_1 - \delta_2. \quad (\text{S9})$$

At optimality $J^*(\mathbf{K}) = \min_{\beta, b} J(\beta, b; \mathbf{K})$ and $J_{\text{rob}}^* = \min_{\xi, \beta, b} J_{\text{rob}}(\xi, \beta, b; \mathbf{K}^*)$ to get (34). Eliminating $\xi \geq 0$ from the constraints (S6) give us the hinge-loss form of the objective used in Eq. (35). \square

C. Second-order cone programming

A second-order cone program (SOCP) involves a linear objective function with one or more second-order cone constraints and any additional linear inequality constraints. An example of a second-order cone constraint in $d + 1$ dimensions is $\|x\|_2 \leq t$, where $\mathbf{x} \in \mathbb{R}^d$, $t \in \mathbb{R}$. The convex approximations we developed for the chance constraints (chance-1) and (chance-2), i.e. (S6) and (S8) respectively, are second-order cone representable. This was shown for the chance constraint approach involving the SVM Dual in Ref. [13]. We show it for the SVM Primal (ROB-PRIMAL) below.

The constraint (S6) can be represented as a second-order cone (SOC) constraint by simply introducing an additional variable r with the SOC constraint $\|\beta\| \leq r$, and replacing $\|\beta\|$ by r in (S6) which is an additional linear inequality constraint. Similarly, (S8) is a quadratic constraint which can be straight-forwardly expressed as a SOC constraint $\|A\beta\| \leq t$, where $A \in \mathbb{S}_+^m$ is the positive-definite square root of the matrix $A^2 = \left(\mathbf{K}^* + \frac{c}{2\sqrt{N}} \kappa(\delta_2) I \right) \in \mathbb{S}_+^m$. The primal objective (PRIMAL-2) along with the linear and SOC constraints stated above forms a second-order cone program (SOCP) which can be solved efficiently [28]. We use the MOSEK solver for its numerical implementation in Python using the convex programming package `cvxpy`.